

Enhancement of Metal–Metal Coupling at a Considerable Distance by Using 4-Pyridinealdazine as a Bridging Ligand in Polynuclear Complexes of Rhenium and Ruthenium

Mauricio Cattaneo, Florencia Fagalde, and Néstor E. Katz*

Instituto de Química Física, Facultad de Bioquímica, Química y Farmacia, Universidad Nacional de Tucumán, Ayacucho 491, (T4000INI) San Miguel de Tucumán, Argentina

Ana María Leiva

Facultad de Química, Pontificia Universidad Católica de Chile, Casilla 306, Santiago, Chile

Russell Schmehl

Department of Chemistry, Tulane University, New Orleans, Louisiana 70118

Received August 2, 2005

Novel polynuclear complexes of rhenium and ruthenium containing PCA (PCA = 4-pyridinecarboxaldehyde azine or 4-pyridinealdazine or 1,4-bis(4-pyridyl)-2,3-diaza-1,3-butadiene) as a bridging ligand have been synthesized as PF_6^- salts and characterized by spectroscopic, electrochemical, and photophysical techniques. The precursor mononuclear complex, of formula $[\text{Re}(\text{Me}_2\text{bpy})(\text{CO})_3(\text{PCA})]^+$ (Me_2bpy = 4,4'-dimethyl-2,2'-bipyridine), does not emit at room temperature in CH_3CN , and the transient spectrum found by flash photolysis at $\lambda_{\text{exc}} = 355$ nm can be assigned to a MLCT (metal-to-ligand charge transfer) excited state $[(\text{Me}_2\text{bpy})(\text{CO})_3\text{Re}^{\text{II}}(\text{PCA}^-)]^+$, with $\lambda_{\text{max}} = 460$ nm and $\tau < 10$ ns. The spectral properties of the related complexes $\{[\text{Re}(\text{Me}_2\text{bpy})(\text{CO})_3\text{PCA}]^{2+}, [\text{Re}(\text{CO})_3(\text{PCA})_2\text{Cl}], \text{ and } [\text{Re}(\text{CO})_3\text{Cl}]_3(\text{PCA})_4$ confirm the existence of this low-energy MLCT state. The dinuclear complex, of formula $[(\text{Me}_2\text{bpy})(\text{CO})_3\text{Re}^{\text{I}}(\text{PCA})\text{Ru}^{\text{II}}(\text{NH}_3)_5]^{3+}$, presents an intense absorption in the visible spectrum that can be assigned to a MLCT $d_{\pi}(\text{Ru}) \rightarrow \pi^*(\text{PCA})$; in CH_3CN , the value of $\lambda_{\text{max}} = 560$ nm is intermediate between those determined for $[\text{Ru}(\text{NH}_3)_5(\text{PCA})]^{2+}$ ($\lambda_{\text{max}} = 536$ nm) and $[(\text{NH}_3)_5\text{Ru}(\text{PCA})\text{Ru}(\text{NH}_3)_5]^{4+}$ ($\lambda_{\text{max}} = 574$ nm), indicating a significant decrease in the energy of the π^* -orbital of PCA. The mixed-valent species, of formula $[(\text{Me}_2\text{bpy})(\text{CO})_3\text{Re}^{\text{I}}(\text{PCA})\text{Ru}^{\text{III}}(\text{NH}_3)_5]^{4+}$, was obtained in CH_3CN solution, by bromine oxidation or by controlled-potential electrolysis at 0.8 V in a OTTLE cell of the $[\text{Re}^{\text{I}},\text{Ru}^{\text{II}}]$ precursor; the band at $\lambda_{\text{max}} = 560$ nm disappears completely, and a new band appears at $\lambda_{\text{max}} = 483$ nm, assignable to a MMCT band (metal-to-metal charge transfer) $\text{Re}^{\text{I}} \rightarrow \text{Ru}^{\text{III}}$. By using the Marcus–Hush formalism, both the electronic coupling (H_{AB}) and the reorganization energy (λ) for the metal-to-metal intramolecular electron transfer have been calculated. Despite the considerable distance between both metal centers (~ 15.0 Å), there is a moderate coupling that, together with the comproportionation constant of the mixed-valent species $[(\text{NH}_3)_5\text{Ru}(\text{PCA})\text{Ru}(\text{NH}_3)_5]^{5+}$ ($K_c \sim 10^2$, in CH_3CN), puts into evidence an unusual enhancement of the metal–metal coupling in the bridged PCA complexes. This effect can be accounted for by the large extent of “metal–ligand interface”, as shown by DFT calculations on free PCA. Moreover, λ is lower than the driving force $-\Delta G^\circ$ for the recombination charge reaction $[\text{Re}^{\text{II}},\text{Ru}^{\text{II}}] \rightarrow [\text{Re}^{\text{I}},\text{Ru}^{\text{III}}]$ that follows light excitation of the mixed-valent species. It is then predicted that this reverse reaction falls in the Marcus inverted region, making the heterodinuclear $[\text{Re}^{\text{I}},\text{Ru}^{\text{III}}]$ complex a promising model for controlling the efficiency of charge-separation processes.

Introduction

Asymmetric polynuclear complexes, and in particular the heterodinuclear mixed-valent complexes of the type $\text{X}_5\text{M}-$

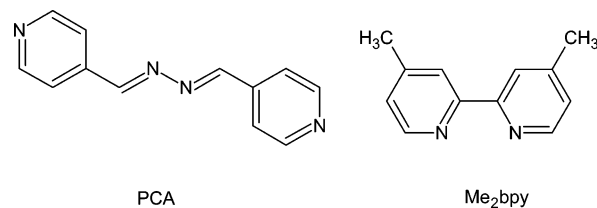
* To whom correspondence should be addressed. E-mail: nkatz@arnet.com.ar.

$\text{L}-\text{M}'\text{X}'_5$ (M = metal with electronic configuration d^6 ; M' = metal with electronic configuration d^5 ; L = bridging ligand; X and X' = coligands), are simple models for simulating the primary photosynthetic processes and for increasing the efficiency of photoelectrochemical cells.¹

We have recently described² new heterodinuclear complexes of the type [(bpy)(CO)₃Re^I(L)Ru^{III}(NH₃)₅]⁴⁺, with bpy = 2,2'-bipyridine and L = 4,4'-bpy (=4,4'-bipyridine), 4-CNpy (=4-cyanopyridine), and BPE (=trans-1,2-bis(4-pyridyl)ethene), and predicted that, only for those complexes exhibiting high redox asymmetries and moderate metal-metal distances, the recombination processes that follow the intervalence optical transitions fall in the Marcus inverted region, making these species promising materials for building energy conversion devices.

To improve the efficiency of the primary charge separation processes, we report in this work the syntheses and characterization of novel polynuclear complexes of rhenium and ruthenium using Re(Me₂bpy)(CO)₃⁺ (Me₂bpy = 4,4'-dimethyl-2,2'-bipyridine) as a photosensitizing unit, Ru(NH₃)₅ⁿ⁺ as electron donor (*n* = 2) or acceptor (*n* = 3) groups, and PCA (PCA = 4-pyridinecarboxaldehyde azine or 4-pyridinealdazine or 1,4-bis(4-pyridyl)-2,3-diaza-1,3-butadiene) as a bridging ligand. For comparison purposes, rhenium complexes having PCA but not Me₂bpy in their coordination spheres have also been prepared and characterized, as well as ammine ruthenium complexes with PCA. Tricarbonyl complexes of Re^I have been extensively studied in connection to photochemical electron and energy transfer processes.³ The ligand PCA, on the other hand, has been used for connecting metallic centers in polymeric structures;⁴ a good electronic communication is expected, considering the electron delocaliza-

Chart 1



tion promoted by including free N atomic orbitals in the bridge. The structures of the ligands are shown in Chart 1.

Experimental Section

Materials and Techniques. All used chemicals were pa. CH₃-CN was distilled over P₄O₁₀. Tetrakis(*n*-butyl)ammonium hexafluorophosphate (TBAH) was purified by repeated recrystallization over ethanol and dried at 150 °C for 72 h. IR spectra were measured (as KBr pellets) by using a double-beam Perkin-Elmer 983G spectrophotometer. UV-vis spectra were recorded on Shimadzu UV-160A and Varian Cary 50 spectrophotometers, provided with 1-cm cells. Electrochemical measurements were carried out in CH₃CN (0.1 M TBAH) with a BAS Epsilon electrochemical equipment. A standard three-electrode compartment cell was used with Ag/AgCl (3 M KCl) as a reference electrode, Pt or vitreous C as working electrodes, and Pt wire as an auxiliary electrode. All values of redox potentials, *E*_{1/2}, were referred to Ag/AgCl. Spectroelectrochemical experiments were performed in a OTTE (optically transparent thin layer electrolysis) type cell from BAS. Emission studies were made by employing a Shimadzu RF-5301 PC spectrofluorometer, provided with 1-cm fluorescence cells. A nanosecond Photonics instrument, with a Quantel Brilliant laser with around 4 ns pulses and 25–30 mJ/pulse, was used for the flash photolysis experiments. Ar was bubbled through the solutions for 15 min prior to electrochemical and photophysical measurements. ¹H and ¹³C NMR spectra were determined in CD₃CN solutions (SiMe₄ as internal reference) with a Bruker Avance 400 MHz spectrometer. Chemical analyses for C, H, and N were done at INQUIMAE, University of Buenos Aires, Buenos Aires, Argentina, with an error of ±0.5%. Density functional theory (DFT) calculations were carried out with a Gaussian98 program package,⁵ using optimization with B3LYP/6-311G bases, within a spin-restricted formalism.

Syntheses. PCA. The ligand 4-pyridinealdazine was prepared as described previously.^{4f} Anal. Found: C, 68.4; N, 25.9; H, 5.8. Calcd for C₁₂H₁₀N₄: C, 68.6; N, 26.6; H, 4.8. This ligand tends to absorb atmospheric water, introducing more error in the % H. IR (KBr, cm⁻¹): 1627 (m), 1594 (s), 1551 (m), 1417 (s), 1309 (s), 1235 (s), 1208 (w), 1082 (w), 1058 (w), 987 (w), 976 (m), 958 (w), 875 (w), 814 (s), 678 (s), 510 (s), 445 (w). UV-vis in CH₃-CN [λ_{max} , nm (10⁻³ ϵ_{max} , M⁻¹ cm⁻¹): 276 (29.0), 286 (29.0), 297 (sh), 310 (sh).

- (1) (a) Balzani, V.; Scandola, F. *Supramolecular Photochemistry*; Ellis Horwood: Chichester, U.K., 1991. (b) Balzani, V.; Juris, A.; Venturi, M.; Campagna, S.; Serroni, S. *Chem. Rev.* **1996**, *96*, 759. (c) Argazzi, R.; Bignozzi, C. A.; Heimer, T. A.; Meyer, G. J. *Inorg. Chem.* **1997**, *36*, 2. (d) Kleverlaan, C. J.; Indelli, M. T.; Bignozzi, C. A.; Pavanin, L.; Scandola F.; Hasselman, G. M.; Meyer, G. J. *J. Am. Chem. Soc.* **2000**, *122*, 2840. (d) Dürr, H.; Bossmann, S. *Acc. Chem. Res.* **2001**, *34*, 905.
- (2) (a) Fagalde, F.; Katz, N. E. *J. Coord. Chem.* **2001**, *54*, 367. (b) Mellace, M. G.; Fagalde, F.; Katz, N. E. *Polyhedron* **2003**, *22*, 369.
- (3) (a) Wrighton, M.; Morse, D. L. *J. Am. Chem. Soc.* **1974**, *96*, 998. (b) Westmoreland, T. D.; Schanze, K. S.; Neveux, P. E., Jr.; Danielson, E.; Sullivan, B. P.; Chen, P.; Meyer, T. J. *Inorg. Chem.* **1985**, *24*, 2596. (c) Kalyanasundaram, K. *J. Chem. Soc., Faraday Trans.* **1986**, *2*, 2401. (d) Chen, P.; Westmoreland, T. D.; Danielson, E.; Schanze, K. S.; Anthon, D.; Neveux, P. E., Jr.; Meyer, T. J. *Inorg. Chem.* **1987**, *26*, 1116. (e) Chen, P.; Danielson, E.; Meyer, T. J. *J. Phys. Chem.* **1988**, *92*, 3708. (f) Juris, A.; Campagna, S.; Bidd, I.; Lehn, J.-M.; Ziessel, R. *Inorg. Chem.* **1988**, *27*, 4007. (g) Sullivan, B. P. *J. Phys. Chem.* **1989**, *93*, 24. (h) Kaim, W.; Kramer, H. E. A.; Vogler, C.; Reiker, J. *J. Organomet. Chem.* **1989**, *367*, 107. (i) Wallace, L.; Jackman, D. C.; Rillema, D. P.; Merkert, J. W. *Inorg. Chem.* **1995**, *34*, 5210. (j) Berger, S.; Klein, A.; Kaim, W.; Fiedler, J. *Inorg. Chem.* **1998**, *37*, 5664. (k) Abbott, L. C.; Arnold, C. J.; Ye, T.-Q.; Gordon, K. C.; Perutz, R. N.; Hester, R. E.; Moore, J. N. *J. Phys. Chem.* **1998**, *102*, 1252. (l) Striplin, D. R.; Crosby, G. A. *Coord. Chem. Rev.* **2001**, *211*, 163. (m) Dattelbaum, D. M.; Itokazu, M. K.; Murakami Iha, N. Y.; Meyer, T. J. *J. Phys. Chem. A* **2003**, *107*, 4092. (n) Wenger, O. S.; Henling, L. M.; Day, M. W.; Winkler, J. R.; Gray, H. B. *Inorg. Chem.* **2004**, *43*, 2043. (o) Pomestchenko, I. E.; Polyansky, D. E.; Castellano, F. N. *Inorg. Chem.* **2005**, *44*, 3412.
- (4) (a) Raj, S. S. S.; Fun, H.-K.; Zhang, J.; Xiong, R. G.; You, X.-Z. *Acta Crystallogr.* **2000**, *C56*, e274. (b) Dong, Y.-B.; Smith, M. D.; zur Loye, H.-C. *J. Solid State Chem.* **2000**, *155*, 143. (c) Baer, A. J.; Macartney, D. H. *Inorg. Chem.* **2000**, *39*, 1410. (d) Dong, Y.-B.; Smith, M. D.; Layland, R. C.; zur Loye, H.-C. *Chem. Mater.* **2000**, *12*, 1156. (e) Dong, Y.-B.; Smith, M. D.; zur Loye, H.-C. *Inorg. Chem.* **2000**, *39*, 4927. (f) Ciurtin, D. M.; Dong, Y.-B.; Smith, M. D.; Barclay, T.; zur Loye, H.-C. *Inorg. Chem.* **2001**, *40*, 2825. (g) Shi, Y.-J.; Li, L.-H.; Li, Y.-Z.; Xu, Y.; Chen, X.-T.; Xue, Z.; You, X.-Z. *Inorg. Chem. Commun.* **2002**, 1090. (h) Gao, E.-Q.; Yue, Y.-F.; Bai, S.-Q.; He, Z.; Yan, C.-H. *J. Am. Chem. Soc.* **2004**, *126*, 1419.

- (5) Frisch, M. J.; Trucks, G. W.; Schlegel, H. B.; Scuseria, G. E.; Robb, M. A.; Cheeseman, J. R.; Zakrzewski, V. G.; Montgomery, J. A., Jr.; Stratmann, R. E.; Burant, J. C.; Dapprich, S.; Millam, J. M.; Daniels, A. D.; Kudin, K. N.; Strain, M. C.; Farkas, O.; Tomasi, J.; Barone, V.; Cossi, M.; Cammi, R.; Mennucci, B.; Pomelli, C.; Adamo, C.; Clifford, S.; Ochterski, J.; Petersson, G. A.; Ayala, P. Y.; Cui, Q.; Morokuma, K.; Malick, D. K.; Rabuck, A. D.; Raghavachari, K.; Foresman, J. B.; Cioslowski, J.; Ortiz, J. V.; Stefanov, B. B.; Liu, G.; Liashenko, A.; Piskorz, P.; Komaromi, I.; Gomperts, R.; Martin, R. L.; Fox, D. J.; Keith, T.; Al-Laham, M. A.; Peng, C. Y.; Nanayakkara, A.; Gonzalez, C.; Challacombe, M.; Gill, P. M. W.; Johnson, B. G.; Chen, W.; Wong, M. W.; Andres, J. L.; Head-Gordon, M.; Replogle, E. S.; Pople, J. A. *Gaussian 98*, revision A.6; Gaussian, Inc.: Pittsburgh, PA, 1998.

[Re(Me₂bpy)(CO)₃(PCA)]PF₆·H₂O (1) and [(Me₂bpy)(CO)₃Re^I(PCA)Re^I(CO)₃(Me₂bpy)](PF₆)₂·2H₂O (2). A 100 mL round-bottom flask was filled with 200 mg (0.0553 mmol) of Re(CO)₅Cl and 40 mL of methylene chloride. AgPF₆ (152 mg; 0.0601 mmol) was dissolved in 5 mL of methanol and added to the flask, and the mixture was stirred in the dark under argon for 18 h at room temperature. The formed AgCl was removed by suction filtration. The filtrate was placed in a 100 mL round-bottom flask, and 165 mg (0.0885 mmol) of Me₂bpy was added. The mixture was stirred in the dark under Ar for 10 h at room temperature. The resulting solution was then filtered and evaporated to dryness; 25 mL of methanol was then added, and the solution was again filtered and evaporated to dryness. The solid material remaining in the flask was dissolved in 50 mL of methylene chloride and placed in a 100 mL round-bottom flask, and 116 mg (0.0553 mmol) of PCA was added. The mixture was stirred in the dark for 18 h at room temperature under argon. The solution was then evaporated to dryness. The solid material remaining in the flask was dissolved in a minimum amount of 1:4 (v/v) acetonitrile/methylene chloride, sorbed onto a silica gel (75/230 mesh) column, and eluted with the same solvent. The yellow fractions (the first is **2** and the second is **1**) were evaporated to dryness, redissolved in acetone, and precipitated with ether. For complex **1**: yield, 109 mg (24%). Anal. Found: C, 39.7; H, 3.2; N, 9.7. Calcd for C₂₇H₂₄N₆O₄PF₆Re: C, 39.2; H, 2.9; N, 10.1. IR (KBr, cm⁻¹): 2032 (s), 1918 (s); 1618 (m), 1597 (w), 1553 (w), 1487 (w), 1419 (m), 1309 (w), 1241 (w), 1031 (w), 844 (s), 738 (w), 688 (w), 646 (w), 628 (w), 556 (m). ¹H NMR (CD₃CN; δ (ppm)) of Me₂bpy: 9.03 (d, 2H, J₅₋₆ = 5.73 Hz, H₆); 8.22 (s, 2H, H₃); 7.60 (d, 2H, J₅₋₆ = 5.72 Hz, H₅); 2.55 (s, 3H, Me). ¹H NMR (CD₃CN; δ (ppm)) of PCA: 8.70 (d, 2H, J₂₋₃ = 4.51 Hz, H₂); 8.45 (s, H₄); 8.42 (s, H₄); 8.32 (d, 2H, J₂₋₃ = 5.19 Hz, H₂); 7.69 (d, 2H, J₂₋₃ = 4.47 Hz, H₃); 7.64 (d, 2H, J₂₋₃ = 5.20 Hz, H₃). For complex **2**: yield, 80 mg (20%). Anal. Found: C, 35.2; H, 3.1; N, 7.0. Calcd for C₄₂H₃₈N₈O₈P₂F₁₂Re₂: C, 34.9; H, 2.7; N, 7.7. IR (KBr, cm⁻¹): 2032 (s), 1918 (s); 1618 (m), 1489 (w), 1420 (w), 1309 (w), 1242 (w), 843 (s), 696 (w), 558 (m).

[(Me₂bpy)(CO)₃Re^I(PCA)Ru^{II}(NH₃)₅](PF₆)₃·(CH₃)₂CO·H₂O (3). A 40 mg (0.0494 mmol) amount of **1** was stirred in 10 mL of acetone under Ar for 30 min, and [Ru(NH₃)₅(H₂O)](PF₆)₂ (24 mg, 0.0485 mmol), prepared as reported in the literature,^{6a} was added, followed by continuous stirring under Ar for 2 h in the dark. A 100 mL volume of ethyl ether was added to precipitate the complex, which was dissolved in acetonitrile and purified by chromatography on Sephadex LH-20, using acetonitrile as the eluting solvent. The first blue fraction was collected, evaporated to dryness, redissolved in acetone, precipitated with ether, filtered out, and dried in a vacuum over P₄O₁₀. Yield: 35 mg (53%). Anal. Found: C, 26.1; H, 3.3; N, 10.7. Calcd for C₃₀H₄₅O₅N₁₁F₁₈P₃ReRu: C, 26.5, H, 3.3, N, 11.3. IR (KBr, cm⁻¹): 2032 (s), 1918 (s); 1619 (m), 1491 (w), 1421 (w), 1285 (w), 1240 (w), 1192 (w), 1009 (w), 843 (s), 736 (w), 645 (w), 558 (m). ¹H NMR (CD₃CN; δ (ppm)) of Me₂bpy: 9.03 (d, 2H, J₅₋₆ = 5.71 Hz, H₆); 8.22 (s, 2H, H₃); 7.60 (d, 2H, J₅₋₆ = 5.72 Hz, H₅); 2.55 (s, 3H, Me). ¹H NMR (CD₃CN; δ (ppm)) of PCA: 8.53 (d, 2H, J₂₋₃ = 6.82 Hz, H₂); 8.52 (s, H₄); 8.47 (s, H₄); 8.32 (d, 2H, J₂₋₃ = 5.19 Hz, H₂); 7.65 (d, 2H, J₂₋₃ = 6.82 Hz, H₃); 7.55 (d, 2H, J₂₋₃ = 6.72 Hz, H₃).

[(Me₂bpy)(CO)₃Re^I(PCA)Ru^{III}(NH₃)₅]⁴⁺ (4). The mixed-valent ion was generated in situ by controlled-potential electrolysis or by adding either bromine or *p*-fluorobenzene–diazonium hexafluorophosphate^{2b} to a acetonitrile solution of **3**. The oxidation progress

was monitored by measuring the absorbance changes in the 200–1100 nm range.

[Ru(NH₃)₅(PCA)](PF₆)₂·4H₂O (5). A suspension of PCA (212 mg, 1.01 mmol) in 15 mL of acetone was stirred and bubbled with Ar for 30 min, and [Ru(NH₃)₅(H₂O)](PF₆)₂ (50 mg, 0.101 mmol) was added, followed by continuous stirring under Ar for 2 h in the dark. The desired complex was precipitated with toluene, cooled, filtered out, and dried. It was redissolved in acetone and precipitated with ethyl ether, filtered out, and dried in a vacuum over P₄O₁₀. Yield: 55 mg (79%). Anal. Found: C, 18.5; H, 2.6; N, 17.2. Calcd for C₁₂H₃₃F₁₂N₉O₄P₂Ru: C, 19.0; H, 4.4; N, 16.6. It has been stated before that microanalyses tend to be unreliable for ruthenium amines.^{6b} IR (KBr, cm⁻¹): 1624 (m), 1602 (m), 1576 (w), 1515 (w), 1494 (w), 1423 (w), 1280 (m), 1194 (w), 1016 (w), 849 (s), 750 (w), 634 (w), 558 (m).

[(NH₃)₅Ru(PCA)Ru(NH₃)₅](PF₆)₄ (6). A solution of PCA (11 mg, 0.05 mmol) in 10 mL of acetone was stirred and bubbled with Ar for 30 min, and [Ru(NH₃)₅(H₂O)](PF₆)₂ (50 mg, 0.101 mmol) was added, followed by continuous stirring under Ar for 2 h in the dark. The solid that precipitated with ethyl ether was dissolved in acetonitrile, sorbed onto a Sephadex LH-20 column, and eluted with acetonitrile. The first blue fraction was concentrated in a rotavap at room temperature, precipitated with ethyl ether, filtered out, and dried in a vacuum over P₄O₁₀. This species was only characterized in solution.

[Ru(NH₃)₅(PCA)]³⁺ (7). This complex was generated in situ by adding stoichiometric amounts of bromine to an acetonitrile solution of **5**.

[(NH₃)₅Ru^{II}(PCA)Ru^{III}(NH₃)₅]⁵⁺ (8) and [(NH₃)₅Ru^{III}(PCA)Ru^{III}(NH₃)₅]⁶⁺ (9). These species were generated in situ by spectrophotometric titration of a solution of **6** in acetonitrile using bromine as an oxidant.

[Re(CO)₃(PCA)₂Cl]·CH₂Cl₂ (10). This complex was prepared by refluxing [Re(CO)₅Cl] (60 mg, 0.1659 mmol) with a 10-fold excess of PCA (348 mg, 1.659 mmol) in ~20 mL of toluene for 2 h. After cooling, the formed precipitate was filtered out and washed with copious amounts of toluene. It was then suspended in methylene chloride, sorbed onto a neutral alumina column and eluted by using 1:6 (v/v) acetonitrile/methylene chloride. The intense yellow fraction was collected, rotoevaporated, redissolved in acetone, precipitated with hexane, filtered out, and dried in a vacuum over P₄O₁₀. Yield: 35 mg (29%). Anal. Found: C, 41.6; H, 2.9; N, 13.7. Calcd for C₂₈H₂₂N₈O₃Cl₃Re: C, 41.5; H, 2.7; N, 13.8. IR (KBr, cm⁻¹): 2023 (s), 1913 (s), 1882 (s); 1614 (w), 1596 (w), 1416 (w), 1311 (w), 1232 (w), 1058 (w), 816 (w), 687 (w).

[Cl(CO)₃(PCA)Re^I(PCA)Re^I(CO)₃Cl(PCA)Re^I(PCA)(CO)₃Cl] (11). This trinuclear complex was synthesized by refluxing [Re(CO)₅Cl] (60 mg, 0.1659 mmol) with a 2-fold excess of PCA (69 mg, 0.3286 mmol) in ~50 mL of hexane for 1 h. The precipitate was collected and washed with copious amounts of hot hexane. It was then dissolved in 1:1 (v/v) acetonitrile/methylene chloride and chromatographed in an alumina column with the same solvent as eluent. The first yellow fraction was evaporated, precipitated with hexane, filtered out, and dried in a vacuum under P₄O₁₀. Yield: 55 mg (57%). Anal. Found: C, 38.4; H, 2.8; N, 12.7. Calcd for C₅₇H₄₀N₁₆O₉Cl₃Re₃: C, 38.9; H, 2.3; N, 12.7. IR (KBr, cm⁻¹): 2023 (s), 1915 (s), 1885 (s); 1614 (w), 1596 (w), 1417 (w), 1309 (w), 1234 (w), 1061 (w), 816 (w), 687 (w).

Results and Discussion

Syntheses and IR Characterization. One-pot synthetic procedures were devised to obtain mono- and dinuclear

(6) (a) Sutton, J. E.; Taube, H. *Inorg. Chem.* **1981**, *20*, 3125. (b) Richardson, D. E.; Taube, H. *J. Am. Chem. Soc.* **1983**, *105*, 40.

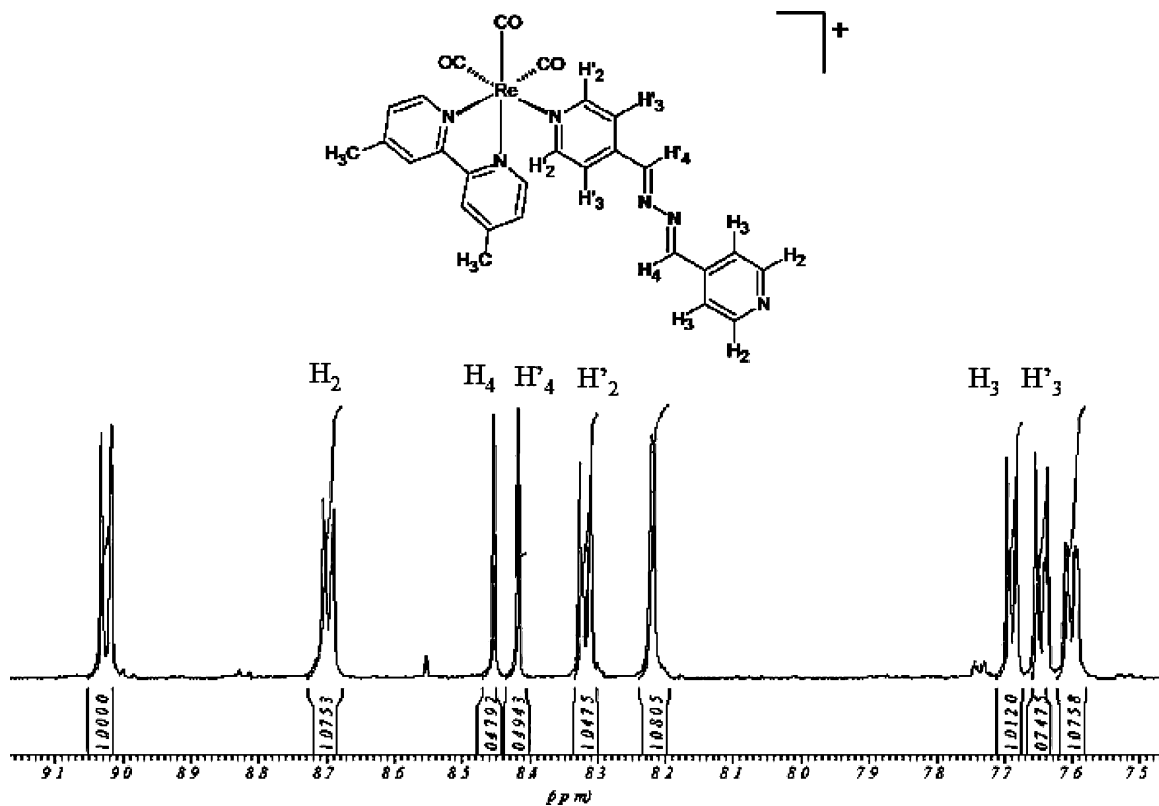


Figure 1. $^1\text{H-NMR}$ spectrum of **1**, in CD_3CN , at 400 MHz.

species of rhenium with PCA, by modifying techniques already described in the literature for similar complexes.⁷ For the heterodinuclear rhenium–ruthenium complexes, we followed procedures previously developed in our laboratory.² In the case of the ammineruthenium species, well-established protocols with some modifications in the purification steps were carried out.⁶ The new complexes were soluble in acetonitrile; their purity was confirmed by chemical analyses, IR, and/or NMR spectra. Thus, in the IR spectra of all rhenium complexes, two intense bands are observed in the region $2100\text{--}1800\text{ cm}^{-1}$, corresponding to the carbonyl stretching frequencies, $\nu_{\text{C}=\text{O}}$. This result is the expected one for a facial configuration of carbonyl groups with local C_{3v} symmetry. Moreover, the values of $\nu_{\text{C}=\text{O}}$ for complexes **1–3** (2032 and 1918 cm^{-1}) are almost the same as those reported for related complexes of the type $\text{fac-}[\text{Re}(\text{bpy})(\text{CO})_3(\text{L})]\text{PF}_6$, with $\text{L} = 4,4'\text{-bpy}$ ($=4,4'$ -bipyridine), 4-CNpy ($=4$ -cyanopyridine), and BPE ($=\text{trans-1,2-bis(4-pyridil)ethene}$),² and $\text{fac-}[\text{Re}(\text{phen})(\text{CO})_3(\text{BPE})]\text{PF}_6$, with $\text{phen} = 1,10$ -phenanthroline.⁸ It can thus be inferred that the bridging ligand PCA does not differ substantially in its π -accepting properties from other nitrogen aromatic heterocycles. The values of $\nu_{\text{C}=\text{O}}$ in complexes **10** (2023 and 1913 cm^{-1}) and **11** (2023 and 1915 cm^{-1}) are definitively lower than those found in the previous complexes, indicating that the introduction of a π -donor group such as chloride (instead of a π -accepting ligand such as PCA) significantly increases the amount of π -back-

bonding from Re^{I} to the carbonyl groups. Similar values of $\nu_{\text{C}=\text{O}}$ have been reported for $[\text{Re}(\text{Me}_2\text{bpy})(\text{CO})_3\text{Cl}]$ and $\text{fac-}[\text{Re}(\text{phen})(\text{CO})_3\text{Cl}]$.⁹ On the other hand, the typical ammonia deformation frequencies, $\delta_{\text{sym}}(\text{NH}_3)$, that appear at 1285 cm^{-1} in **3**, 1280 cm^{-1} in **5**, and at 1287 cm^{-1} in **6** are consistent with localized oxidation states (II) for all ruthenium centers in these complexes.¹⁰

NMR Spectra. Figure 1 shows the NMR spectrum of complex **1**. Due to the symmetry of free PCA, three signals were observed at $\delta = 8.71$ (H_2), 7.87 (H_3), and 8.67 (H_4) ppm. The coordination to the rhenium center results in the loss of symmetry, and six signals were observed for coordinated PCA. The main effect was the shift to high fields of δ for H_2' (8.32 ppm), H_3' (7.64 ppm), and the bridge proton H_4' (8.42 ppm). Only two of the remaining protons show a shift of δ to high fields, H_4 (8.45 ppm) and H_3 (7.69 ppm), that evidences the effect of metal coordination. The H–H COSY spectrum allowed the complete assignment of the signals, as described in the Experimental Section.

The ^1H NMR spectrum of the dinuclear complex **3** shows that the protons of the pyridine ring coordinated to Re remain unaltered with respect to complex **1**, but the H_2 and H_3 protons of the pyridine ring coordinated to Ru are shifted to $\delta = 8.53$ and 7.55 ppm, respectively. The singlets corresponding to the protons of the bridging $\text{C}=\text{N}-\text{N}=\text{C}$ moiety are shifted to $\delta = 8.47$ ppm (H_4' , closer to Re) and

(7) Shaver, R. J.; Perkovic, M. W.; Rillema, D. P.; Woods, C. *Inorg. Chem.* **1995**, *34*, 5446.

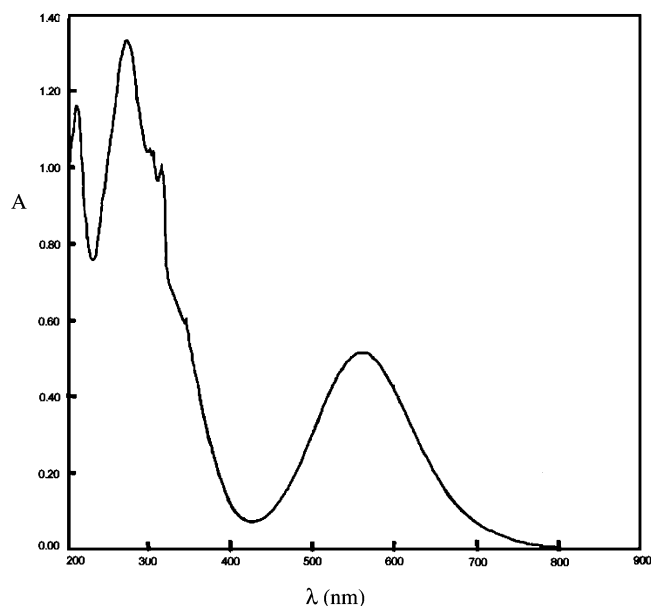
(8) Itokazu, M. K.; Sarto Polo, A.; Araújo de Faria, D. L.; Bignozzi, C. A.; Murakami Iha, N. Y. *Inorg. Chim. Acta* **2001**, *313*, 149.

(9) (a) Worl, L. A.; Duesing, R.; Chen, P.; Della Ciana, L.; Meyer, T. J. *J. Chem. Soc., Dalton Trans.* **1991**, 849. (b) Martí, A. A.; Mezei, G.; Maldonado, L.; Parolitici, G.; Raptis, R. G.; Colón, J. L. *Eur. J. Inorg. Chem.* **2005**, 118.

(10) Fagalde, F.; Katz, N. E. *Polyhedron* **1995**, *14*, 1213.

Table 1. Electronic Absorption Spectral Data, in CH₃CN, at 22 °C

complex	λ_{\max} , nm ($10^{-3}\epsilon_{\max}$, M ⁻¹ cm ⁻¹)
[Re(Me ₂ bpy)(CO) ₃ (PCA)] ⁺ (1)	330 (13.3), 315 (25.2), 302 (27.9), 274 (32.1), 213 (24.4)
[(Me ₂ bpy)(CO) ₃ Re(PCA)Re(CO) ₃ (Me ₂ bpy)] ²⁺ (2)	336 (19.1), 315 (26.8), 303 (27.0), 268 (32.7), 214 (32.5)
[(Me ₂ bpy)(CO) ₃ Re ^I (PCA)Ru ^{II} (NH ₃) ₅] ³⁺ (3)	560 (12.7), 330 (15.6), 316 (25.6), 302 (25.8), 273 (33.1), 212 (30.5)
[(Me ₂ bpy)(CO) ₃ Re ^I (PCA)Ru ^{III} (NH ₃) ₅] ⁴⁺ (4)	483 (1.9) 330 (15.6), 316 (25.6), 302 (25.8), 273 (33.1)
[Ru(NH ₃) ₅ (PCA)] ²⁺ (5)	536 (13.8), 276 (20.4)
[(NH ₃) ₅ Ru ^{II} (PCA)Ru ^{II} (NH ₃) ₅] ⁴⁺ (6)	574 (24.7), 274 (20.4)
[Ru(NH ₃) ₅ (PCA)] ³⁺ (7)	404 (1.9), 330, (sh), 276 (20.4)
[(NH ₃) ₅ Ru ^{II} (PCA)Ru ^{III} (NH ₃) ₅] ⁵⁺ (8)	558 (12.1), 330 (sh), 275 (20.4)
[(NH ₃) ₅ Ru ^{III} (PCA)Ru ^{III} (NH ₃) ₅] ⁶⁺ (9)	465 (4.4), 330 (sh), 276 (20.4)
[ClRe(CO) ₃ (PCA) ₂] ^a (10)	340 (24.7), 281 (62.4)
[Cl(CO) ₃ (PCA)Re(PCA)Re(CO) ₃ Cl(PCA)Re(PCA)(CO) ₃ Cl] ^a (11)	348 (38.7), 280 (96.6)

^a In CH₂Cl₂.**Figure 2.** UV–visible spectra of **3**, in CH₃CN. $C = 3.9 \times 10^{-5}$ M.

to 8.52 ppm (H₄, closer to Ru), indicating a higher π -back-bonding effect from Ru than from Re to the bridging ligand.

UV–Visible Spectra. Table 1 shows the electronic spectral data for all complexes in CH₃CN. UV absorptions between 200 and 300 nm can be assigned to characteristic intraligand $\pi \rightarrow \pi^*$ transitions of the Me₂bpy and PCA ligands.¹¹ Figure 2 shows the UV–visible spectra of the dinuclear Re^I–Ru^{II} species **3**. The mononuclear complex **1** presents an intense absorption of minimum energy at $\lambda_{\max} = 330$ nm that can be assigned¹¹ to two overlapped metal-to-ligand charge transfers (MLCT), $d_{\pi}(\text{Re}) \rightarrow \pi^*(\text{Me}_2\text{bpy})$ and $d_{\pi}(\text{Re}) \rightarrow \pi^*(\text{PCA})$, since both transitions are expected to fall at nearly the same energy. In effect, while most of complexes of the type [Re^I(diimine)(CO)₃(L)]⁺⁰ (L = aromatic nitrogen heterocycle or Cl) have strong absorptions at $\lambda_{\max} \sim 330\text{--}380$ nm due to $d_{\pi}(\text{Re}) \rightarrow \pi^*(\text{diimine})$ MLCT bands,^{2,12} both the mononuclear species **10** and the trinuclear species **11** exhibit intense absorptions at $\lambda_{\max} = 340$ and 348 nm, respectively, in CH₂Cl₂ (see Table 1), which can readily be assigned to $d_{\pi}(\text{Re}) \rightarrow \pi^*(\text{PCA})$ MLCT bands, since only the Re^I–PCA chromophore is present in these latter complexes.

In the homodinuclear Re^I–Re^I complex, **2**, this same band is red-shifted to $\lambda_{\max} = 336$ nm, indicating moderate interaction between both Re centers, similar to that previously reported for [(Me₂bpy)(CO)₃Re^I(4,4'-bpy)Re^I(CO)₃(Me₂bpy)]²⁺.¹¹ The heterodinuclear Re^I–Ru^{II} complex, **3**, has this same MLCT band at $\lambda_{\max} = 330$ nm and a new and intense band at $\lambda_{\max} = 560$ nm, attributed to the MLCT $d_{\pi}(\text{Ru}) \rightarrow \pi^*(\text{PCA})$. This latter value is intermediate between that determined for the mononuclear ruthenium(II) complex, **5** ($\lambda_{\max} = 536$ nm), and the dinuclear diruthenium(II) species, **6** ($\lambda_{\max} = 574$ nm), as shown in Table 1. A significant decrease in the energy of the π^* -orbital of the bridging PCA is then disclosed in the Re^I–Ru^{II} complex **3**.

The long-wavelength absorptions of complexes **5** and **6**, as compared to other ammineruthenium species,^{6,13} can be accounted for by the strong $d_{\pi}(\text{Ru}) \rightarrow \pi^*(\text{PCA})$ π -back-bonding effect caused by the extra π -delocalization pathways introduced by the conjugated $-\text{C}=\text{N}-\text{N}=\text{C}-$ chain of PCA.

Figure 3 shows a spectrophotometric redox titration of the dinuclear decaammine diruthenium complex **6** with Br₂ in CH₃CN. In the mixed-valent species **8**, the $d_{\pi}(\text{Ru}) \rightarrow \pi^*(\text{PCA})$ MLCT band appears at $\lambda_{\max} = 558$ nm, displaced to a longer wavelength respect to the value of the same band in the mononuclear pentaammineruthenium complex **5**, as expected because of its higher charge and electronic delocalization. The metal-to-metal charge transfer (MMCT) transition $d_{\pi}(\text{Ru}^{\text{II}}) \rightarrow d_{\pi}(\text{Ru}^{\text{III}})$ was not detected up to 1100 nm. It has been noted before that the intervalence transitions were increasingly ill-resolved when introducing several conjugated double bonds between the pyridine rings in mixed-valent complexes of the (NH₃)₅Ru(py-) series.^{13c} In the completely oxidized Ru^{III}–Ru^{III} complex **9**, a new band appears at $\lambda_{\max} = 465$ nm, assignable to a ligand-to-metal charge transfer (LMCT) $\pi(\text{PCA}) \rightarrow d_{\pi}(\text{Ru}^{\text{III}})$, by comparison to a similar band previously observed at $\lambda_{\max} = 424$ nm in [Ru(NH₃)₅(4,4'-dpa)]²⁺ (4,4'-dpa = 4,4'-dipyridylamine);⁶ the corresponding band in the mononuclear pentaammineruthenium(III) species **7** appears with less intensity at a shorter wavelength ($\lambda_{\max} = 404$ nm, obtained by Gaussian deconvolution). These results were also reproduced by spectroelectrochemistry of **6** in an OTTE cell.

(11) Tapolsky, G.; Duesing, R.; Meyer, T. J. *Inorg. Chem.* **1990**, *29*, 2285.
 (12) Lees, A. *Chem. Rev.* **1987**, *87*, 711.

(13) (a) Lavalley, D. K.; Fleischer, E. B. *J. Am. Chem. Soc.* **1972**, *94*, 2583.
 (b) Woitellier, S.; Launay, J. P.; Spangler, C. W. *Inorg. Chem.* **1989**, *28*, 758. (c) Launay, J. P. *Chem. Soc. Rev.* **2001**, *30*, 386.

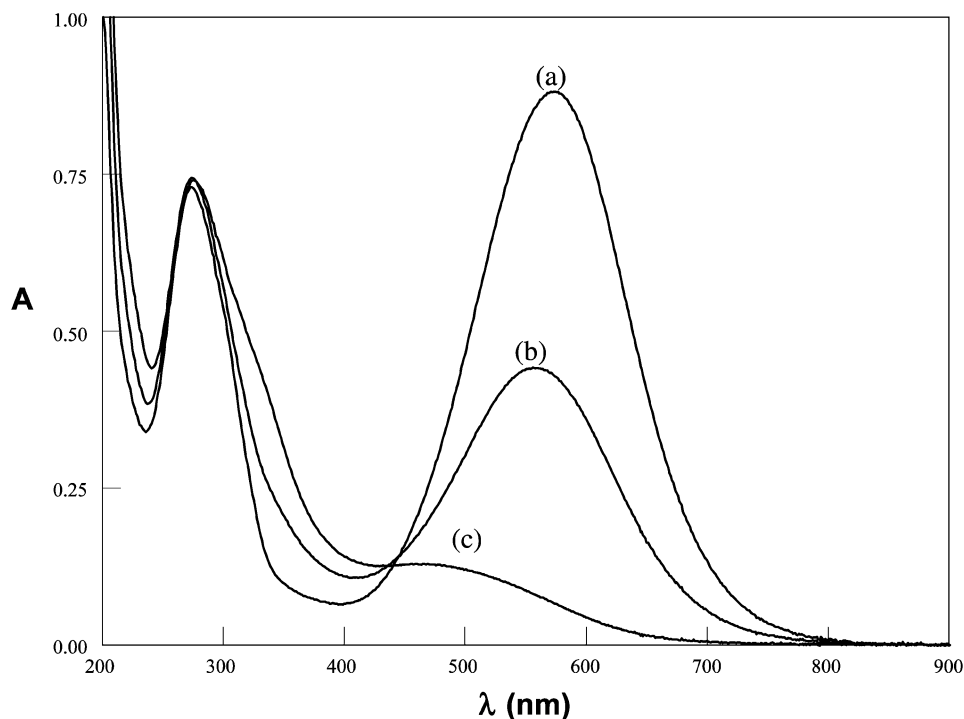


Figure 3. UV–visible absorption spectra in CH_3CN of (a) $[(\text{NH}_3)_5\text{Ru}^{\text{II}}(\text{PCA})\text{Ru}^{\text{II}}(\text{NH}_3)_5]^{4+}$, (b) $[(\text{NH}_3)_5\text{Ru}^{\text{II}}(\text{PCA})\text{Ru}^{\text{III}}(\text{NH}_3)_5]^{5+}$, and (c) $[(\text{NH}_3)_5\text{Ru}^{\text{III}}(\text{PCA})\text{Ru}^{\text{III}}(\text{NH}_3)_5]^{6+}$. $C = 3.7 \times 10^{-5}$ M.

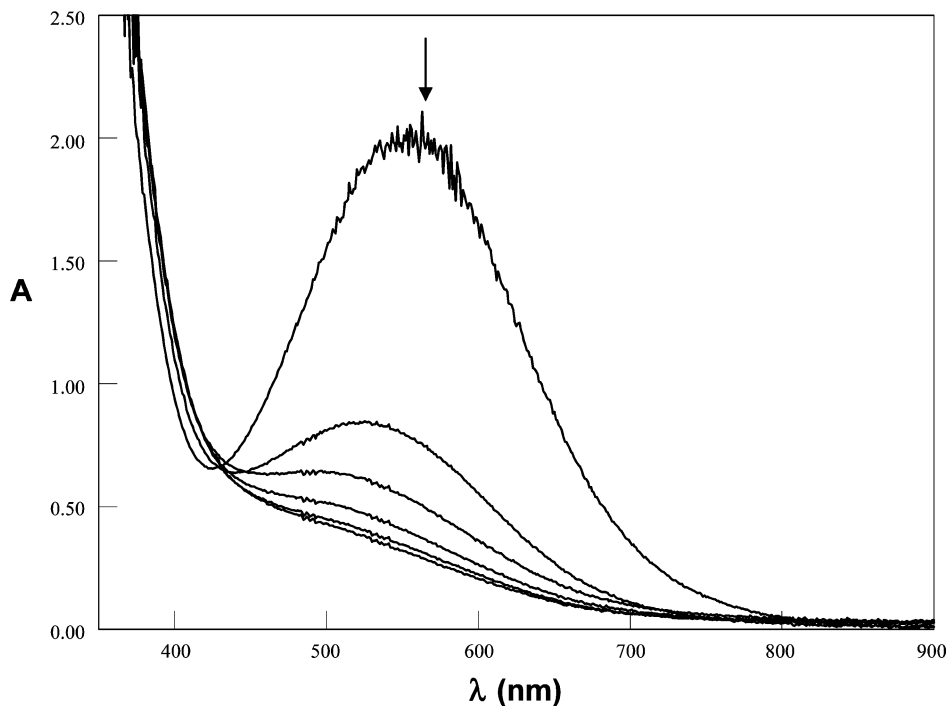


Figure 4. Controlled-potential electrolysis of $[(\text{Me}_2\text{bpy})(\text{CO})_3\text{Re}^{\text{I}}(\text{PCA})\text{Ru}^{\text{II}}(\text{NH}_3)_5]^{3+}$ in an OTTLE cell, in CH_3CN , at 22°C . $C = 1.6 \times 10^{-4}$ M. The arrow indicates increasing times: $t = 0, 2, 4, 6, 8,$ and 10 min.

A controlled-potential electrolysis of the dinuclear $\text{Re}^{\text{I}}\text{—Ru}^{\text{II}}$ species **3** is observed in Figure 4. The band corresponding to $d_{\pi}(\text{Ru}) \rightarrow \pi^*(\text{PCA})$ MLCT at $\lambda_{\text{max}} = 560$ nm disappears completely, indicating the formation of the mixed-valent $\text{Re}^{\text{I}}\text{—Ru}^{\text{III}}$ complex **4**. The new band at $\lambda_{\text{max}} = 483$ nm in this latter species (value obtained by Gaussian deconvolution) can be assigned to a MMCT $\text{Re}^{\text{I}} \rightarrow \text{Ru}^{\text{III}}$, with some contribution from a LMCT $\text{PCA} \rightarrow \text{Ru}^{\text{III}}$ band expected near 400 nm, as detected in the mononuclear

complex **7**. This assignment is confirmed by considering the data obtained previously for the analogous species $[(\text{bpy})(\text{CO})_3\text{Re}^{\text{I}}(\text{L})\text{Ru}^{\text{III}}(\text{NH}_3)_5]^{4+}$ ($\text{L} = 4,4'\text{-bpy, BPE}$), for which no LMCT bands were expected in the 400–500 nm region and only the MMCT bands at $\lambda_{\text{max}} \sim 480$ nm could be observed.² These results are also consistent with maximum wavelength values obtained when oxidizing complex **3** chemically, by adding either bromine or *p*-fluorobenzene-diazonium hexafluorophosphate in CH_3CN . The isobestic

Table 2. Electrochemical Data in CH₃CN, at 22 °C

complex	process	$E_{1/2}$ (V) (ΔE_p , mV) ^a
[Re(Me ₂ bpy)(CO) ₃ (PCA)] ⁺ (1)	Re ^{2+/+}	1.79 (111)
	PCA ^{0/-}	-0.79 (188)
	Me ₂ bpy ^{0/-}	-1.30 (124)
	Re ⁺⁰	-1.68 (irr)
[(Me ₂ bpy)(CO) ₃ Re(PCA)Re(CO) ₃ (Me ₂ bpy)] ²⁺ (2)	Re ^{2+/+}	1.80 (123)
	PCA ^{0/-}	-0.79 (irr)
	Me ₂ bpy ^{0/-}	-1.35 (56)
	Re ⁺⁰	-1.49 (irr)
[(Me ₂ bpy)(CO) ₃ Re ^I (PCA)Ru ^{II} (NH ₃) ₅] ³⁺ (3)	Re ^{2+/+}	1.80 (122)
	Ru ^{3+/2+}	0.47 (76)
	PCA ^{0/-}	-0.78 (irr)
	Me ₂ bpy ^{0/-}	-1.32 (irr)
	Re ⁺⁰	-1.52 (irr)
	Ru ^{3+/2+}	0.43 (69)
[Ru(NH ₃) ₅ (PCA)] ²⁺ (5)		0.22 (irr.)
[(NH ₃) ₅ Ru ^{II} (PCA)Ru ^b (NH ₃) ₅] ⁴⁺ (6)	PCA ^{0/-}	-1.18 (irr)
	Ru _{a,b} ^{3+/2+}	0.44 (103)
		0.20 (irr)

^a All CV data were obtained at $\nu = 100$ mV/s, except for complex **6** ($\nu = 300$ mV/s).

point in Figure 4 is not quite sharp, which may be due to some leakage in the OTTLE cell; ligand isomerization can be discarded, since this process is undetected on the cyclic voltammetry scale (vide infra).

Electrochemistry. Table 2 shows the electrochemical data for the studied complexes. The redox potential for the Re^{II}/Re^I couple of the mononuclear Re^I species **1**, the Re^I–Re^I dinuclear species **2**, and the Re^I–Ru^{II} dinuclear species **3** are very similar (with $E_{1/2}$ ca. 1.80 V, as expected for carbonyl diimine rhenium(I) complexes),² although a chemical transformation occurs in complex **1** after oxidation: a new wave develops at $E_{1/2} \sim 1.50$ V, which may be due to a redox-induced isomerization of PCA from a trans- to a cis-structure, similar to that observed for the mononuclear Ru^{II} species **5**, which will be discussed below. No evidence for this isomerization has been found in the dinuclear complexes **2** and **3**, leading to the conclusion that the metal–metal interaction through the bridging PCA stabilizes the trans-structure.

The ligand PCA is reduced irreversibly at $E_{1/2} \sim -0.8$ V in all complexes. The same effect was found before for the first ligand reduction in the complex [(Me₂bpy)Re^I(CO)₃(pyAm-Mepy⁺)]²⁺ (pyAm-Mepy⁺ = *N*-(4-pyridyl)- β -(*N*-methylpyridinium-3-yl)acrylamide), which was explained by polymerization of pyridyl radicals.¹⁴ For the rhenium complexes, the first reduction of Me₂bpy appears at $E_{1/2} \sim -1.3$ V, while a second irreversible reduction at $E_{1/2} \sim -1.5$ V can be attributed to a Re^{I/0} couple.^{14,15} Introducing the –C=N–N=C– chain between two pyridyl moieties makes the PCA ligand more electron accepting than Me₂bpy. Similar phenomena have been observed before in [Re(MQ⁺)(CO)₃(Me₂bpy)]²⁺ (MQ⁺ = *N*-methyl-4,4'-bipyridinium)¹⁶ and in

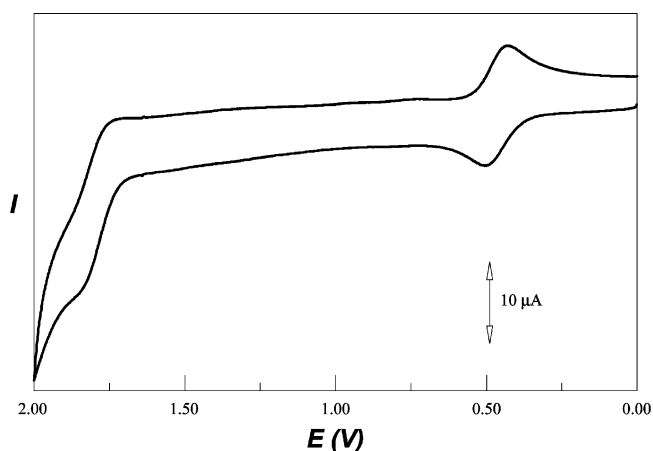


Figure 5. Cyclic voltammogram of [(Me₂bpy)(CO)₃Re^I(PCA)-Ru^{II}(NH₃)₅]³⁺, in the oxidative range, in CH₃CN, 0.1 M TBAH, with $\nu = 200$ mV/s.

[(4-O₂NC₆H₄CO₂)Re(CO)₃(bpy)];¹⁷ these changes should be reflected in the photophysical behavior, which will be discussed later, in the corresponding section.

Figure 5 shows the CV of the asymmetric Re^I–Ru^{II} dinuclear complex **3** in the oxidative range. The new reversible voltammetric wave, absent in complex **1**, that appears at $E_{1/2} = 0.46$ V can be readily assigned to the Ru^{III}/Ru^{II} couple, since this value is similar to those corresponding to the same couple in related complexes² and to the pentaammineruthenium(II) and decaamminediruthenium(II) species **5** and **6** (vide infra). The difference between the redox potentials of both metallic couples in **3** is $\Delta E_{1/2} = E_{1/2}(\text{Re}^{\text{I}}/\text{Re}^{\text{I}}) - E_{1/2}(\text{Ru}^{\text{III}}/\text{Ru}^{\text{II}}) = 1.33$ V.

The mononuclear pentaammineruthenium complex **5** shows a CV typical of linkage isomerization processes,¹⁸ as shown in Supporting Information Figure S1. There is a reversible wave with $E_{1/2} = 0.43$ V that can be assigned to the Ru^{III}/Ru^{II} couple, as discussed previously. When PCA is coordinated to metals in low oxidation states, a zigzag trans-

(14) (a) Katz, N. E.; Mecklenburg, S. L.; Meyer, T. J. *Inorg. Chem.* **1995**, *34*, 1282. (b) Brühlmann, U.; Hayon, E. *J. Am. Chem. Soc.* **1974**, *96*, 6169.

(15) Lin, R.; Fu, Y.; Brock, C. P.; Guarr, T. F. *Inorg. Chem.* **1992**, *31*, 4346.

(16) (a) Chen, P.; Danielson, E.; Meyer, T. J. *J. Phys. Chem.* **1988**, *92*, 3708. (b) Chen, P.; Curry, M.; Meyer, T. J. *Inorg. Chem.* **1989**, *28*, 2271. (c) Mecklenburg, S. L.; Opperman, K. A.; Chen, P.; Meyer, T. J. *J. Phys. Chem.* **1996**, *100*, 15145. (d) Liard, D. J.; Vlček, A., Jr. *Inorg. Chem.* **2000**, *39*, 485.

(17) Feliz, M.; Ferraudi, G. *Inorg. Chem.* **1998**, *37*, 2801.

(18) (a) Katz, N. E.; Fagalde, F. *Inorg. Chem.* **1993**, *32*, 5391. (b) Toma, H. E.; Rocha, R. C. *Croat. Chem. Acta* **2001**, *74*, 499.

structure is preferred.⁴ The broad irreversible cathodic wave with a peak at $E \sim 0.20$ V (at $v = 200$ mV/s) may be assigned to conformers with different structures (probably a cis-isomer that is rapidly converted into another isomer with Ru^{III} bonded to one of the N atoms of the $-\text{C}=\text{N}-\text{N}=\text{C}-$ chain). The Ru^{II} forms of this last isomer are expected to be unstable, so that no anodic wave are detected, at least during the first cycles. A redox-induced isomerization can then be postulated. An additional proof resulted from a simple spectroscopic experiment. After oxidation of complex **5** with bromine to obtain complex **7**, SnCl₂ was added to the solution: the band at $\lambda_{\text{max}} = 536$ nm, attributed to a MLCT in the trans-isomer, was not totally recovered, indicating some irreversibility.

Supporting Information Figure S2 shows some ill-resolved waves for both Ru^{III}/Ru^{II} couples in the dinuclear decaammine complex **6** at a average value of $E_{1/2} = 0.44$ V, slightly higher than the mononuclear precursor **5**, as expected for an increased charge. The peak-to-peak separation is large (103 mV), indicating metal–metal electronic coupling comparable to the mixed-valent species⁶ $[(\text{NH}_3)_5\text{Ru}(4,4'\text{-dpa})\text{Ru}(\text{NH}_3)_5]^{5+}$. Although experimental evidence on all PCA complexes reported up to now point to the trans-structure as the most stable one for this ligand,⁴ and the obtained values of the redox potentials are consistent with this structure, a ligand isomerization process, similar to that described before for complex **5**, can be detected after oxidizing both ruthenium atoms (Figure S2). Besides, the voltammograms of both complexes **5** and **6** were reproducible only by polishing the working electrode after each measurement, since adsorption and polymerization processes tend to occur.

The comproportionation constant K_c for complex **8** can be determined from the following equation:¹⁹

$$K_c = 10^{(\Delta E/0.059)} \quad (1)$$

Here ΔE is the observed difference in redox potentials for the [Ru^{III/II}] couples.

With an estimated difference of $\Delta E \sim 0.12$ V, the obtained value, $K_c \sim 10^2$, is indicative of a metal–metal interaction unexpectedly strong when considering the distance between both metallic centers, estimated as $r \sim 14.9$ Å, from the crystallographic data for the free ligand PCA^{4d} and related Ru complexes.²⁰ A similar value of K_c has been determined for the 4,4'-dipyridylamine analogue,⁶ despite its much shorter metal–metal distance ($r \sim 10.9$ Å). We therefore confirm previous findings that distance and size do not always define the behavior in mixed-valence chemistry: for example, the complex $[(\text{NC})_4\text{Fe}(\text{bptz})\text{Fe}(\text{CN})_4]^{3-}$ (bptz = 3,6-bis(2-pyridyl)-1,2,4,5-tetrazine) has a much stronger metal–metal coupling than the bpm-bridged analogue (bpm = 2,2'-bipyrimidine), although the metal–metal distance is longer.²¹ A DFT calculation on the ligand PCA indicates that the LUMO, shown in Figure 6, is almost

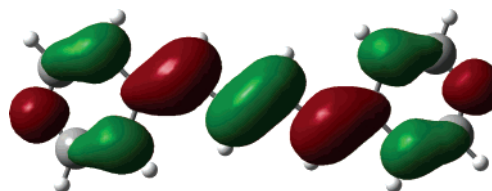


Figure 6. LUMO for free PCA obtained from a DFT calculation.

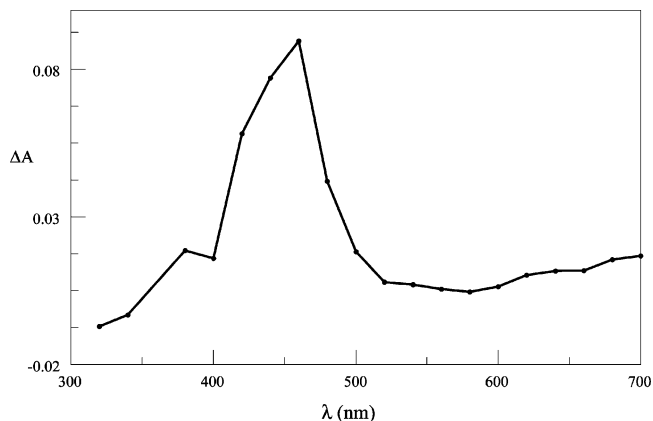


Figure 7. Transient absorption difference spectrum of **1** in CH₃CN at 22 °C acquired 19 ns after laser excitation at $\lambda_{\text{exc}} = 355$ nm. $C = 2 \times 10^{-4}$ M.

completely delocalized and has very strong contributions of the coordinating N, enhancing the extent of “metal–ligand interface”. The N p_z orbitals will overlap well with metal d_{xz} orbitals, assuming that x is the metal–metal axis and the z axis is perpendicular to the plane of the ligand.

Photophysical Properties. All the spectroscopic and electrochemical data analyzed in the preceding sections indicate that PCA is a better π -accepting ligand than Me₂-bpy. Therefore, a fast deactivation of the $d_{\pi}(\text{Re})-\pi^*(\text{Me}_2\text{-bpy})$ MLCT excited state to a low-lying $d_{\pi}(\text{Re})-\pi^*(\text{PCA})$ can be anticipated. In effect, all complexes studied in this work do not emit in CH₃CN solutions at room temperature, except for complex **2**, which presents a weak emission at $\lambda_{\text{max}} = 538$ nm ($\lambda_{\text{exc}} = 336$ nm), typical of Re^{II}(diimine⁻) complex MLCT excited states.² For complex **1**, the transient spectrum obtained in CH₃CN by laser flash photolysis at $\lambda_{\text{exc}} = 355$ nm has a maximum at $\lambda_{\text{max}} = 460$ nm and a lifetime $\tau < 10$ ns (Figure 7). Moreover, the transient spectrum does not resemble what one would expect for a Re^{II}-Me₂bpy⁻ CT excited state ($\lambda_{\text{max}} = 370$ nm)²² but instead is very similar to that obtained when exciting $[(\text{Me}_2\text{-bpy})\text{Re}^{\text{I}}(\text{CO})_3(\text{pyAm-Mepy}^+)]^{2+}$ with a laser light at $\lambda_{\text{exc}} = 420$ nm; the band that appeared at $\lambda_{\text{max}} = 455$ nm was attributed to a pyridyl radical bonded to Re^{II}.^{14a} For example, the nicotinamide and *N*-methylnicotinamide radicals, obtained by pulse radiolysis, absorb at $\lambda_{\text{max}} = 445$ nm in aqueous solutions.^{14b} The quenching of the luminescence of complex **1** can thus be explained by crossing to this $[(\text{Me}_2\text{bpy})(\text{CO})_3\text{Re}^{\text{II}}(\text{PCA}^-)]^+$ excited state, which is not so efficient in complex **2**. Quenching of luminescence from Re → diimine MLCT excited states by crossing to lower

(19) (a) Ernst, S.; Kasack, V.; Kaim, W. *Inorg. Chem.* **1988**, *27*, 1146. (b) Kaim, W.; Kasack, V. *Inorg. Chem.* **1990**, *29*, 4696. (c) Kaim, W.; Klein, A.; Glöckle, M. *Acc. Chem. Res.* **2000**, *33*, 755.

(20) Shin, Y.-K.; Szalda, D. J.; Brunschwig, B. S.; Creutz, C.; Sutin, N. *Inorg. Chem.* **1997**, *36*, 3190.

(21) Glöckle, M.; Kaim, W.; Katz, N. E.; García Posse, M.; Cutin, E. H.; Fiedler, J. *Inorg. Chem.* **1999**, *38*, 3270.

(22) Stufkens, D. J.; Vlček, A., Jr. *Coord. Chem. Rev.* **1998**, *177*, 127.

lying Re → BL MLCT excited states (BL = bridging ligand) has been previously reported in related complexes.¹⁵ This assignment is further supported by 77 K luminescence data. Both complexes **1** and **2** have emission maxima at 525 nm in ethanol/methanol glasses, as shown in Supporting Information Figure S3. The emission energy is similar to that of related Re^I diimine complexes having pyridine or CH₃CN as the sixth ligand (i.e. in [(diimine)(CO)₃ReL]⁺ complexes, L = π-accepting ligand). The observation is also consistent with the fact that, at room temperature, the one electron oxidation and reduction potentials are nearly the same in both **1** and **2**. Earlier work of Gray and co-workers on [Re(Me₂-bpy)(CO)₃(*trans*-bpe)]⁺ (bpe = 1,2-bis(4-pyridyl)ethylene)³ⁿ indicated clearly that the lowest energy excited state in low-temperature matrixes is a bpe ligand localized triplet state. We anticipated the same in this system, but the low-temperature luminescence spectra strongly suggest a ³MLCT emitting excited state even in low-temperature matrixes given the lack of structure in the emission.

Intramolecular Electron Transfer. From a Marcus–Hush formalism and the experimental data of the MMCT transition in the mixed-valence complex **4**,²³ the reorganization energy λ for the intramolecular electron transfer through the PCA bridge can be calculated as

$$\lambda = E_{\text{op}} - \Delta G^{\circ} - \Delta E_{\text{exc}} \quad (2)$$

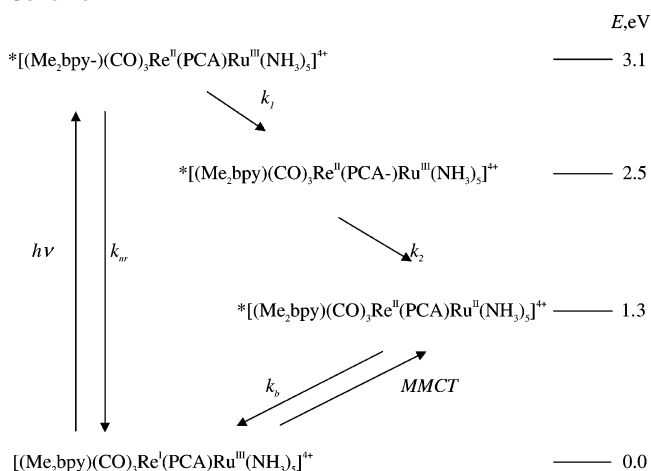
where E_{op} is the energy of the MMCT absorption maximum, ΔG° is the free energy difference between both redox sites, obtained approximately as the difference in the redox potentials $\Delta E_{1/2}$, and ΔE_{exc} is an excited-state energy difference, if we consider that the optical transition leads to an electronically excited state.²⁴ We can also determine the electronic coupling elements H_{AB} through the well-known Hush formula:²⁵

$$H_{\text{AB}} = \frac{2.06 \times 10^{-2}}{r} (\epsilon_{\text{max}} \cdot \Delta \tilde{\nu}_{1/2} \cdot \tilde{\nu}_{\text{max}})^{1/2} \quad (3)$$

Where H_{AB} is the donor–acceptor coupling element (in cm⁻¹), r is the metal–metal distance (in Å), and ϵ_{max} , $\Delta \tilde{\nu}_{1/2}$, and $\tilde{\nu}_{\text{max}}$ are the molar absorptivity (in M⁻¹ cm⁻¹), bandwidth at half-height (in cm⁻¹), and energy maximum of the MMCT band (in cm⁻¹), respectively. Thus, substituting the values of $E_{\text{op}} = 2.57$ eV, $\Delta G^{\circ} = 1.33$ eV, and $\Delta E_{\text{ex}} = 0.25$ eV²⁴ in eq 2, we obtain $\lambda \sim 1$ eV, a value comparable to that obtained before for similar complexes.^{2,26} Since $\lambda < -\Delta G^{\circ}$ (=1.33 eV) for the reverse electron-transfer process [Re^{II},Ru^{II}] → [Re^I,Ru^{III}], we predict that this back-reaction will fall in the Marcus inverted region.²⁷

From eq 3, and considering deconvoluted (and corrected for the LMCT contribution) values of $\tilde{\nu}_{\text{max}}$ (=2.07 × 10⁴ cm⁻¹), ϵ_{max} (=1.9 × 10³ M⁻¹ cm⁻¹), and $\Delta \tilde{\nu}_{1/2}$ (=5.5 × 10³ cm⁻¹), we determine a value of $H_{\text{AB}} = 6.4 \times 10^2$ cm⁻¹, which

Scheme 1



discloses a significant coupling in the mixed-valent asymmetric complex **4**, despite the considerable distance, $r \sim 15.0$ Å (estimated from crystallographic data for PCA^{4f} and related Re complexes¹⁵), that separates both metal centers and in consistency with what was discussed before on the extent of metal–metal interaction in the mixed-valent symmetric diruthenium complex **8**. This value of H_{AB} is similar to that already reported for the analogous complex [(bpy)(CO)₃Re^I-(4,4'-bpy)Ru^{III}(NH₃)₃]⁴⁺² ($H_{\text{AB}} = 7.5 \times 10^2$ cm⁻¹), where the metal–metal distance is 25% shorter ($r = 11.3$ Å). However, and since $H_{\text{AB}} \ll \lambda$, this complex belongs to class II of Robin and Day nomenclature.²⁵

Scheme 1 summarizes the processes that can occur upon light excitation in the dinuclear [Re^I,Ru^{III}] mixed-valence species **4**, a good model for simulating primary charge separation processes relevant in the design of efficient photoconverters.

Conclusions. The bridging ligand PCA allows a significant electronic communication between the metal centers in homo- and heterodinuclear complexes, notwithstanding the considerable metal–metal separation distance. This enhancement is due to the strong electronic delocalization induced by the –C=N–N=C– chain that connects the coordinating pyridyl rings. Moreover, in the [Re^I,Ru^{III}] complex **4**, the reorganization energy λ is less than the driving force $-\Delta G^{\circ}$ for the reverse charge recombination step, [Re^{II},Ru^{II}] → [Re^I,Ru^{III}], that follows light excitation, and so this process is expected to fall in the Marcus inverted region. We conclude that these complexes are promising models for reaching a fine control of the rate of charge separation processes that are relevant in artificial photosynthesis.

Acknowledgment. We thank the UNT, CONICET, ANPCyT (Argentina), and Antorchas Foundation for financial support. DAAD is gratefully acknowledged for a donation of BAS equipment. F.F and N.E.K. are members of the Research Career (CONICET of Argentina). M.C. thanks ANPCyT and CONICET for graduate fellowships. We thank Dr. Barbara Loeb (PUC of Chile) for her help in establishing scientific cooperation between Chile and Argentina and Dr. Miguel A. Blesa (CNEA of Argentina) for helpful suggestions. R.S. thanks the U.S. Department of Energy, Office of

(23) (a) Hush, N. S. *Prog. Inorg. Chem.* **1967**, 8, 391. (b) Hush, N. S. *Coord. Chem. Rev.* **1985**, 64, 135.

(24) Katz, N. E.; Creutz, C.; Sutin, N. *Inorg. Chem.* **1988**, 27, 168.

(25) Creutz, C. *Prog. Inorg. Chem.* **1983**, 30, 1.

(26) Lin, R.; Guarr, T. G. *Inorg. Chim. Acta* **1994**, 226, 79.

(27) Marcus, R. A.; Sutin, N. *Biochim. Biophys. Acta* **1985**, 811, 265.

Chemical Sciences (Grant DE-FG-02-96ER141617), for support of this research.

Supporting Information Available: Crystallographic voltammograms of **5** and **6** and emission spectra of **1** and **2** at 77 K. This

material is available free of charge via the Internet at <http://pubs.acs.org>.

IC051312B